Theoretical study of the high-pressure phase stability of GaP, InP, and InAs

A. Mujica
Departamento de Física Fundamental y Experimental, Universidad de La Laguna, La Laguna E-38205, Tenerife, Spain

R. J. Needs
Theory of Condensed Matter Group, Cavendish Laboratory, University of Cambridge, Cambridge CB3 0HE, United Kingdom
(Received 7 August 1996; revised manuscript received 6 December 1996)

We report a first-principles study of the high-pressure structural properties and phase diagrams of GaP, InP, and InAs. The present study includes the *Cmcm* phase, which is a distortion of the rocksalt structure, and the *Imm2* and sc16 phases, which have been suggested as stable high-pressure phases of III-V compounds. Our work relates directly to recent experimental work on III-V compounds, which has indicated that the previously reported high-pressure phase diagrams of these compounds should be reconsidered. Our results support the existence of stable *Cmcm* phases in InP and InAs and a stable or nearly stable *Cmcm* phase in GaP. We find stable *Imm2* phases in each of the compounds studied. We also find a small range of thermodynamic stability for sc16 GaP. The energy-volume curves and phase diagrams of InP and InAs, as well as those of GaP and GaAs, show remarkable similarities. Along with previous work, we now have enough theoretical results to support a different systematics of the high-pressure phases of III-V compounds. [S0163-1829(97)03215-3]

I. INTRODUCTION

Recent developments in angle dispersive powder x-ray-diffraction techniques as applied to high-pressure experiments have greatly increased the resolution that can be achieved.[1] These improvements have led to a reevaluation of the high-pressure phase diagrams of many materials.[2,3] At the same time the capabilities of first-principles electronic-structure calculations have improved and predictions of new stable high pressure phases have been made. One result of these developments has been the complete rewriting of the high-pressure phase diagrams of some III-V and II-VI compounds.[3,4] No doubt there are more experimental discoveries and theoretical predictions and rationalizations to come.

A remarkable feature of the emerging picture of the high-pressure phases of III-V and II-VI compounds is that the highly symmetrical rocksalt phase, if present, has a smaller range of stability than previously thought and the β-tin structure, which was once thought to be common in these compounds, is now thought to be rather uncommon. Indeed, recent experimental work[5] has indicated that all, or almost all, previously reported occurrences of β-tin phases in III-V compounds are incorrect. The actual phases are now thought to be either an orthorhombic structure referred to as *Cmcm* after its space group or a structure closely related to the β-tin structure known as *Imm2* (see Sec. II) or its site disordered counterpart *Imma*. The *Cmcm* structure can be regarded as a distortion of the rocksalt structure. Being a distortion of the rocksalt structure, the *Cmcm* phase is likely to be stable in those compounds having stable or near stable rocksalt phases. It is therefore desirable to investigate more closely all reports of stable rocksalt phases in III-V and other compounds. Stable *Cmcm* phases have recently been observed in several II-VI and III-V compounds.[1] An early theoretical treatment of a *Cmcm* phase was our study of *Cmcm* GaAs,[6,7] which identified this as the structure of the experimentally observed phase known as GaAs-II. More recently a theoretical study of ZnTe has appeared[8] that supports the experimental finding[3] of a stable *Cmcm* phase in this compound. Recent experimental and theoretical work has raised a number of other questions regarding the high-pressure phase diagrams of these compounds. For example, calculations by Crain *et al.*[10] indicated that under increasing pressure the zinc-blende phases of GaAs, InAs, and AlSb would become unstable to the so-called sc16 phase, which is the binary analogue of the bc8 structure observed as a metastable phase in silicon[11,12] and germanium.[9,13] Although the original calculations[10] were subsequently found to be inaccurate, more careful studies[6] have predicted that sc16 GaAs could in fact be stable over a very small pressure range. Conclusive experimental evidence for the existence of a stable sc16 phase in any III-V compound is, however, still lacking.

In this contribution we have studied the high-pressure phases of GaP, InP, and InAs, taking into consideration recent candidate structures such as sc16 (see Ref. 6) and *Cmcm* and *Imm2* (which are described in Sec. II), along with the well-known zinc-blende (zb), rocksalt (NaCl), cesium chloride (CsCl), β-tin, and nickel arsenide (NiAs) structures.[14] A brief description of the calculations is given in Sec. III. In Sec. IV we report and discuss our results on the phase stability of these compounds with special attention to the *Cmcm* and *Imm2* phases. In Sec. V we present the results for the structural parameters of the phases. Finally, in Sec. VI we draw the conclusions from our study.

II. DESCRIPTION OF THE STRUCTURES

A. The *Cmcm* structure

A brief description of the *Cmcm* structure is given in Refs. 6 and 7 but here we give a more detailed description, introducing the notation that we will use. *Cmcm* has an orthorhombic primitive unit cell containing two *A*-*B* pairs, where *A* and *B* are the atomic species forming the binary

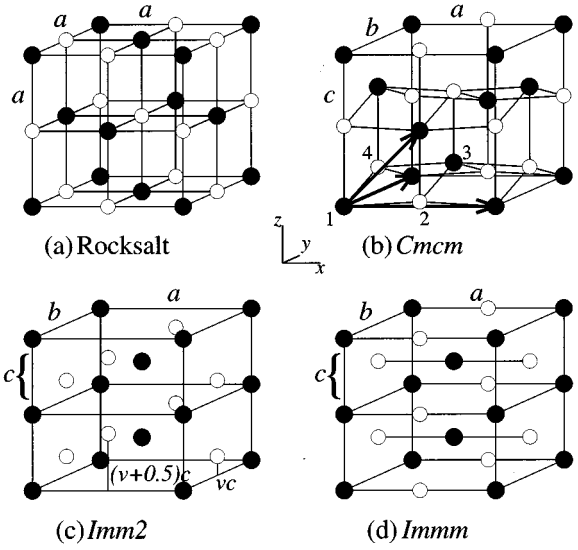

FIG. 1. Representation of the (a) rocksalt, (b) *Cmcm*, (c) *Imm2*, and (d) *Immm* structures. The atoms in the basis of the *Cmcm* structure are labeled 1–4. The lattice generators of the *Cmcm* structure are shown in bold. This picture corresponds to $u=0.35$ and $\delta=0.03$. The *Imm2* structure represented in (c) corresponds to $v=0.25$. When $v=0.5$ the *Imm2* structure becomes the *Immm* structure depicted in (d).

compound. The *Cmcm* structure is depicted in Fig. 1(b). The structure is defined by the three lattice constants a, b, and c, and two internal parameters u_A and u_B, which relate to the positions within the unit cell of one type of atomic species. In a Cartesian coordinate system the translation vectors of *Cmcm* are

$$\mathbf{a}_1=(a,0,0),\quad \mathbf{a}_2=(0,b,0),\quad \mathbf{a}_3=\left(\frac{a}{2},0,\frac{c}{2}\right) \tag{1}$$

and the positions of the four atoms in the unit cell are

$$A:\tau_1=\left(-\frac{a}{4},-\frac{b}{4},-\frac{c}{4}u_A\right),$$

$$B:\tau_2=\left(\frac{a}{4},-\frac{b}{4},-\frac{c}{4}u_B\right),$$

$$A:\tau_3=\left(\frac{a}{4},\frac{b}{4},\frac{c}{4}u_A\right),$$

$$B:\tau_4=\left(-\frac{a}{4},\frac{b}{4},\frac{c}{4}u_B\right). \tag{2}$$

Apart from a change in orientation, an identical structure is obtained by replacing u_A and u_B by $-u_A$ and $-u_B$, respectively, or by replacing u_A and u_B by $2-u_A$ and $2-u_B$, respectively. Thus we may restrict the values of u_A and u_B to lie between 0 and 1.

Figures 1(a) and 1(b) show that the *Cmcm* structure can be constructed from the rocksalt structure by a sequence of distortions consisting of (i) an orthorhombic adjustment of the axes, (ii) a shearing of alternate (010) planes in the [001] direction, and (iii) a puckering of the atomic rows in the [100] direction. With reference to the rocksalt structure, the atoms in *Cmcm* are contained in flat (010) planes, but the rows of atoms along the [100] direction within each plane are slightly puckered. The internal parameters u_A and u_B represent the relative displacement of the alternate (010) planes for each sublattice that is composed of a single atomic species. The net shearing of the planes is measured by the parameter $u=\frac{1}{2}(u_A+u_B)$. The puckering of the atomic rows arises because u_A is not equal to u_B (although in practice their values are close). This puckering is measured by the parameter $\delta=\frac{1}{2}(u_A-u_B)$. The *Cmcm* structure can be described in terms of u_A and u_B or in terms of δ and u. The latter description will be more convenient when we discuss the instability of the rocksalt structure to the shearing and puckering distortions. The undistorted rocksalt structure is obtained when $u_A=u_B=0$ (equivalently, $u=\delta=0$) and $b/a=c/a=1$. If $u_A=u_B$, then $\delta=0$ and the structure is sheared, but the atomic rows are not puckered. If, on the other hand, $u_A=-u_B$, then $u=0$ and the structure is puckered, but not sheared.

The four structural degrees of freedom of *Cmcm* at fixed volume can lead to a variety of different coordination numbers, with bond lengths and the identity of close neighbors depending on the values of the parameters. Experimentally, the coordination number has been found to range from six, in the case of the rocksalt structure, to nearly eight. For $u_A=u_B=0.5$ and proper values for the axial ratios the arrangement of the atomic sites can be made hexagonal (with the c axis in the x direction).[15]

The *Cmcm* structure is related in a simple way to the structure that has been incorrectly referred to as *Amm2*.[16] This structure was once thought to be stable in a variety of II-VI and III-V compounds under pressure. It corresponds to taking $u_A=u_B$ (i.e., $\delta=0$). However, no symmetry consideration can favor δ being zero in binary compounds, as the symmetry is not changed by fixing $\delta=0$ in *Cmcm*, and the structure is in general unstable towards the more general *Cmcm* structure with $\delta\neq 0$.[7] Thus there seems to be no good reason why this degree of freedom should be *a priori* neglected in an analysis of the *Cmcm* structure, although in practice δ is rather small for several compounds (see Sec. V).

B. The *Imm2* structure

The *Imm2* structure is body-centered orthorhombic and its unit cell contains a single *A*-*B* pair. The structure is defined by the three lattice constants a, b, and c and one internal parameter v. The *Imm2* structure is represented in Figs. 1(c) and 1(d) for the two important cases $v=0.25$ and $v=0.5$. In Cartesian coordinates, the translation vectors of *Imm2* are

$$\mathbf{a}_1=\left(-\frac{a}{2},\frac{b}{2},\frac{c}{2}\right),\quad \mathbf{a}_2=\left(\frac{a}{2},-\frac{b}{2},\frac{c}{2}\right),\quad \mathbf{a}_3=\left(\frac{a}{2},\frac{b}{2},-\frac{c}{2}\right) \tag{3}$$

TABLE I. Calculated and experimental values of the equilibrium lattice constant a_0, bulk modulus B_0, and pressure derivative of the bulk modulus B_0' at zero pressure, for the zinc-blende phase of each of the compounds studied.

	GaP		InP		InAs	
	Calc.	Expt.	Calc.	Expt.	Calc.	Expt.
a_0 (Å)	5.411	5.447[a]	5.942	5.869[a]	6.122	6.058[a]
B_0 (Mbar)	0.90	0.91[a]	0.68	0.71[a]	0.56	0.58[a]
B_0'	4.5		4.9		4.6	

[a]Reference 42.

and the positions of the two atoms in the unit cell are

$$A:\tau_1=\left(-\frac{a}{4},-\frac{b}{4},-\frac{c}{2}v\right),$$

$$B:\tau_2=\left(-\frac{a}{4},\frac{b}{4},\frac{c}{2}v\right). \quad (4)$$

As in the case of $Cmcm$, the three independent degrees of freedom of $Imm2$ at fixed volume allow a variety of coordinations that in practice range from nearly six to eight. The following properties of $Imm2$ limit the range of variation of v. Replacing v by $1-v$ leaves the structure unchanged, apart from a reflection in the x-y plane. Also, replacing v by $0.5-v$ together with interchanging the axis lengths a and b leaves the structure unchanged (except for a 90° rotation about the z axis). We may thus restrict v to have values between 0.25 and 0.5.

When $v=0.25$ and $b/a=1$ the symmetry is increased and the $Imm2$ structure becomes the binary analog of the β-tin structure, with the replacement of the two atoms in the monatomic β-tin unit cell by the two different atomic species of the binary compound. When $v=0.5$ the symmetry is again increased and the structure becomes centrosymmetric with space group $Immm$. Note that for $b/c=\sqrt{3}$ and $v=0.5$, the arrangement of the lattice of *sites* is the same as in the monatomic simple hexagonal structure, with the c axis in the x direction. However, when a *crystal* composed of two different atomic species is considered, each occupying one of the two atomic sites of a monatomic simple hexagonal cell in this representation, no extra symmetry is introduced when the axis lengths obey this relation. Thus, contrary to the monatomic case, in the minimum (or maximum) energy structure b and c are not related by any symmetry consideration when $v=0.5$. This fact was apparently neglected in early theoretical[29] and experimental[18] works in which the structure with $v=0.5$ and $b/c=\sqrt{3}$ was considered to be the binary analogue of simple hexagonal. It was assumed that the above relation between lattice constants followed from symmetry considerations in binary compounds and consequently one degree of freedom was omitted from the analysis.

III. CALCULATIONAL DETAILS

The calculations were performed within the framework of the density-functional formalism, using the plane-wave pseudopotential scheme with the Ceperley-Alder form[19] of the local-density approximation (LDA). We used norm-conserving pseudopotentials[20] constructed via the Kerker scheme,[21] which included scalar relativistic effects. For the cation pseudopotentials (Ga^{3+} and In^{3+}) we included nonlinear core-valence exchange-correlation corrections,[22,23,17] which are important for these atoms. For all the calculations reported here we used basis sets containing plane waves up to an energy cutoff of 24 Ry. To resolve the small energy differences between phases very-high-quality Brillouin-zone integrations are required.[24] For the metallic $Cmcm$ and NiAs phases, which both have four atoms per unit cell, we used $12\times12\times14$ and $14\times14\times10$ meshes respectively, referred to the choice of lattice vectors given in Sec. II. For the metallic NaCl, CsCl, and *Imm2* structures, which have two atoms per unit cell, we used $16\times16\times16$ meshes. For the semiconducting zinc-blende phases (two atoms per unit cell) and for sc16 (16 atoms per unit cell) we used $8\times8\times8$ meshes and $4\times4\times4$ meshes, respectively. The forces on the atoms and components of the stress tensor were calculated and used in the relaxation of the structures.[25] The uncertainties in the energy differences between phases due to all numerical approximations (basis set, Brillouin zone integration, relaxation of the structures, etc.) are estimated to be less than 5 meV per formula unit. There are of course additional approximations in our calculations due to the use of the LDA, the pseudopotential approximation, and the neglect of zero-point motion, etc.

The calculated zero-pressure lattice constants and bulk moduli of the zinc-blende phases are given in Table I, along with experimental data. In each case the agreement between the theoretical and experimental values is very good.

IV. STABILITY OF THE PHASES

In Figs. 2, 3, and 4 we show the energy-volume (E-V) curves for the various phases of GaP, InP, and InAs. For the *Imm2* structures, we have plotted only the E-V curves corresponding to $v=0.25$ (β tin) and to $v=0.5$ ($Immm$) (see Sec. IV F). In these graphs the volumes V are given in terms of the theoretical zero-pressure volumes of the zinc-blende phases, which can be obtained from the lattice constants given in Table I. The continuous lines in Fig. 2 are Chebyshev polynomial fits to the calculated data. The estimated error in each fit is less than 10^{-4} eV per formula unit. The energy is given with respect to the calculated energy of the zinc-blende phase at zero pressure. In each figure, graphs (a) and (b) correspond, respectively, to the higher- and lower-volume regions investigated in each compound. Due to the number of structures considered and the closeness of some of the E-V curves, we show in the insets an enlargement of the

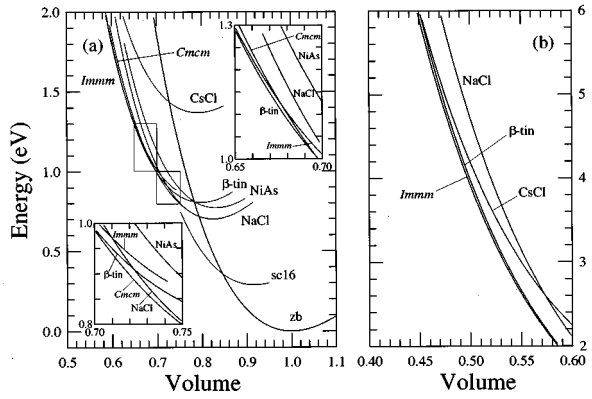

FIG. 2. Energy-volume curves for the various structures considered for GaP. (a) High-volume region. (b) Low-volume region. The energies (in eV per formula unit) are given with respect to the energy of the zinc-blende phase at zero pressure. The volumes are given in terms of the calculated zero-pressure volume of the zinc-blende phase $V_{0,\mathrm{the}}^{\mathrm{GaP}} = 39.61$ Å^3 per formula unit. The insets enlarge the more congested areas of the figures.

more congested areas of each graph.

At each volume, the pressure p was calculated by differentiation of the fitted E-V curves. The values of the pressure calculated in this way are in good agreement with those calculated directly using the stress theorem.[25] The p-V relations for the more important structures of the three compounds considered are plotted in Figs. 5–7(a). The p-V relations are important as, unlike the E-V curves, they can be directly compared with experimental data for the stable phases. The thermodynamically stable phase at a given pressure and temperature is the one with the lowest Gibbs free energy. In our theoretical study we work at zero temperature, so that the relevant thermodynamic potential is the enthalpy $H=E+pV$. Figures 5–7(b) show enthalpy-pressure (H-p) curves for the three compounds. In Table II we summarize the pressures at which the more relevant crossings of the enthalpy curves take place and the value of the volume of each structure at these pressures.

A. GaP

We predict that the zinc-blende structure becomes thermodynamically unstable to sc16 at a pressure of 147 kbar.

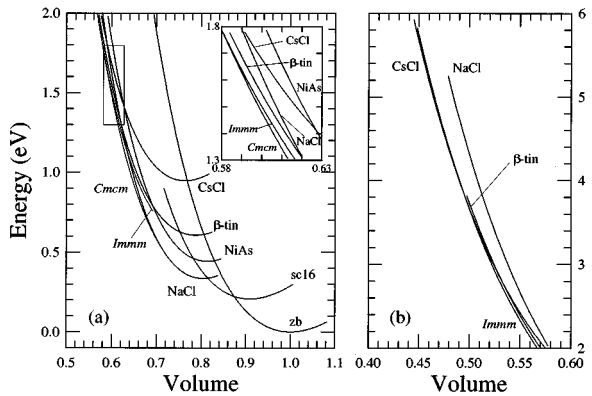

FIG. 3. Same as Fig. 2, but for InP ($V_{0,\mathrm{the}}^{\mathrm{InP}} = 52.46$ Å^3 per formula unit).

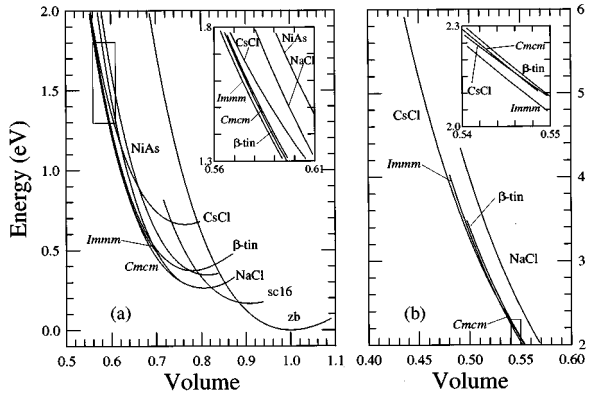

FIG. 4. Same as Fig. 2, but for InAs ($V_{0,\mathrm{the}}^{\mathrm{InAs}} = 57.36$ Å^3 per formula unit).

sc16 GaP is predicted to become unstable to the β-tin structure at 203 kbar and unstable to the $Cmcm$ structure at 204 kbar. These pressures are the same to within the error bars of our calculations and we conclude that these phases are equally stable at these pressures. As the pressure is further increased the β-tin structure becomes more stable than $Cmcm$. At still higher pressure transitions are predicted to the $Immm$ structure at 388 kbar and then to the CsCl structure at a pressure greater than 2500 kbar.

Although $Cmcm$ and $Immm$ GaP were not considered in previous calculations, some comparisons with our results are still possible. For example, García and Cohen[26] calculated that the zinc-blende phase becomes unstable to NaCl at a pressure of 188 kbar, which is close to our calculated value of 183 kbar.

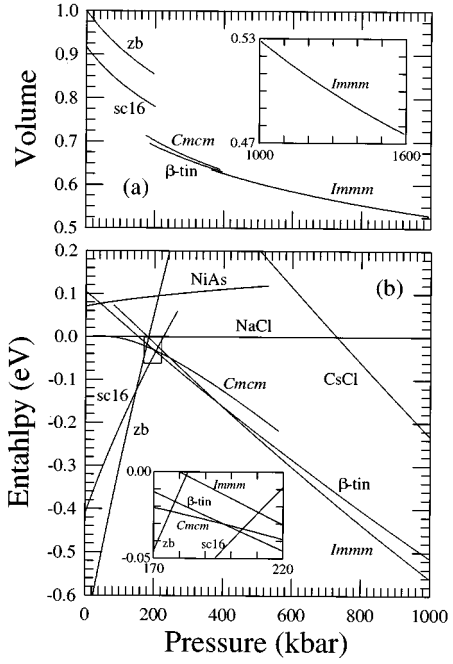

FIG. 5. (a) Volume-pressure and (b) enthalpy-pressure curves for the different structures of GaP investigated. At each pressure the enthalpy is measured with respect to the enthalpy of the rocksalt structure. The more relevant crossings between the H-p curves are summarized in Table II. Only the p-V curves of the more important structures are plotted.

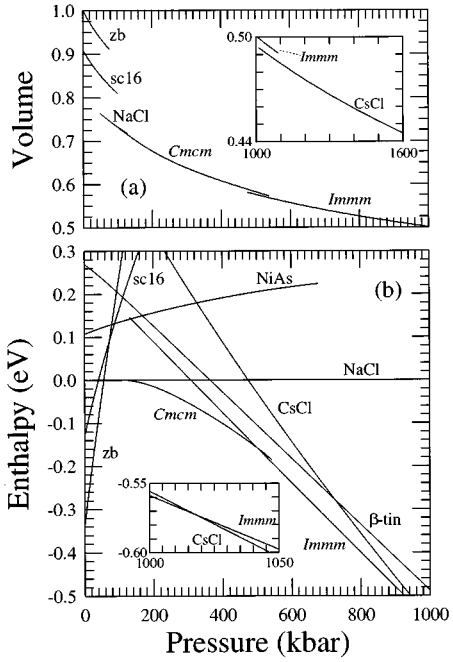

FIG. 6. Same as Fig. 5, but for InP.

Comparison with experiment is complicated by three considerations: (i) many first-order transitions show significant hysteresis due to kinetic effects, so that the onset of the transition does not correspond to the coexistence pressure of the two phases, (ii) if the kinetic barriers are very large a transition may be entirely suppressed, and (iii) some of the very small enthalpy differences between phases are at the limit of the resolution of our calculations. The above predicted sequence of phase stability should be viewed with these facts in mind. First, to date there is no experimental observation of an sc16 phase in any III-V compound, and it has been argued

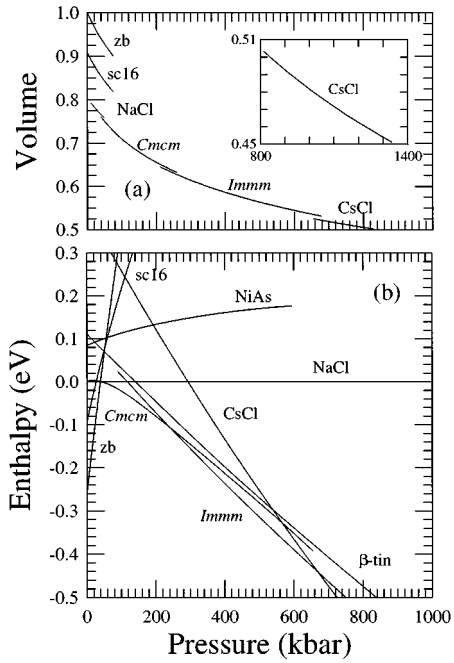

FIG. 7. Same as Fig. 5, but for InAs.

TABLE II. Values of the coexistence pressures p_e at which the enthalpy curves for the different structures shown in Figs. 5–7(b) cross each other. The structure to the right of the arrow (II) is more stable at pressures above the coexistence pressure. Only the more relevant crossings for each compound are listed. The volume per formula unit of each structure at the coexistence pressure is also given.

I→II	p_e (kbar)	V_e^{I} (Å^3)	V_e^{II} (Å^3)
	GaP		
zb→sc16	147	34.96	31.97
zb→*Cmcm*	177	34.30	28.21
zb→β tin	178	34.28	27.64
zb→NaCl	183	34.17	28.65
zb→NiAs	211	33.59	28.38
zb→CsCl	302	32.01	25.50
sc16→*Cmcm*	204	30.84	27.73
sc16→β tin	203	30.85	27.24
Cmcm→β tin	197	27.85	27.33
β-tin→*Immm*	388	25.06	24.94
Immm→CsCl	$\gg$2500	16.76	16.48
	InP		
zb→NaCl	56	48.87	39.87
zb→sc16	73	48.05	43.60
zb→NiAs	80	47.64	39.45
zb→β tin	94	47.02	37.45
zb→CsCl	138	45.27	35.28
NaCl→*Cmcm*	110–120	38.1–37.9	38.1–37.9
Cmcm→*Immm*	503	30.51	30.20
Immm→CsCl	1020	26.15	25.86
	InAs		
zb→NaCl	39	54.02	43.94
zb→sc16	53	53.03	48.16
zb→NiAs	56	52.83	43.64
zb→CsCl	86	51.05	39.76
zb→β tin	51	53.20	42.05
NaCl→*Cmcm*	30–45	44.2–43.7	44.2–43.7
Cmcm→*Immm*	240	36.65	36.38
Immm→CsCl	670	30.56	30.00
Cmcm→CsCl	560	31.72	31.04

that a direct transition from zinc blende to sc16 will not occur in binary compounds because of kinetic considerations.[10] If the transition to a sc16 phase is suppressed by kinetic factors then we predict that the zinc-blende phase would become unstable to the *Cmcm* structure at a pressure of 177 kbar. The predicted volume reduction is large (about 18%). *Cmcm* GaP would then be a *metastable* phase from 177 kbar up to 197 kbar, where it becomes unstable to the β-tin phase. Second, as mentioned above, the *Cmcm* and β-tin phases are close in enthalpy at pressures in the range 150–250 kbar, so that we cannot rule out the existence of a *thermodynamically* stable *Cmcm* phase between the sc16 and β-tin phases [see the inset of Fig. 5(b)]. Third, we do not rule out the existence of a stable *Imm2* phase with v between 0.25 (β tin) and 0.5 (*Immm*). We will comment further on the β-tin→*Immm* transition and the possible stability of an intermediate *Imm2* phase in Sec. IV F.

In early experimental work a transition from zinc blende to a disordered β-tin phase was reported to occur at 215 kbar.[27] However, preliminary experimental studies by Nelmes and McMahon[5] indicate that the β-tin phase is not stable in GaP and that the diffraction pattern of the post-recovered phase is indeed remarkably similar to those for the *Cmcm* phase in a variety of other compounds. Our findings support this preliminary experimental evidence of a stable *Cmcm* phase in GaP. Furthermore, Besson and co-workers[28] have observed irreversible opacity in GaP at about 180 kbar, which is close to our value for the zinc-blende→*Cmcm* transition pressure of 177 kbar. We further predict the stability of β-tin and *Immm* phases at higher pressures. We calculate the *Cmcm*→β-tin transition pressure to be 197 kbar, although this value is subject to an error bar of ± 15 kbar because the enthalpies of these phases are very similar over a large range of pressures. The calculated coexistence pressure of the β-tin and *Immm* phases is 388 ± 20 kbar. Finally, we predict that the *Immm* phase becomes unstable to the CsCl phase at very high pressures, above 2500 kbar. No experimental study of GaP at these high pressures has been reported so far.

B. InP

For InP we predict

$$\text{zinc-blende} \xrightarrow{56\ \text{kbar}} \text{NaCl} \xrightarrow{110-120\ \text{kbar}} Cmcm \xrightarrow{503\ \text{kbar}} Immm \xrightarrow{1020\ \text{kbar}} \text{CsCl}.$$

(The numerical values over the arrows correspond to the calculated pressures at which the enthalpies are equal.)

We have not found a thermodynamically stable sc16 phase for InP. Instead we predict a zinc-blende→rocksalt transition at 56 kbar. This transition pressure is significantly lower than the value of 128 kbar reported in the theoretical study by Zhang and Cohen.[29] We note, however, that these authors did not include nonlinear core-valence exchange-correlation corrections, which are important for In compounds. Calculations by García and Cohen[26] indicate that including these corrections reduces the zinc-blende →rocksalt coexistence pressure by about 60 kbar in GaP and by about 40 kbar in GaAs. Experimentally a transition from zinc-blende to rocksalt has been reported to occur at 105 kbar,[30] which is somewhat above our value. However, we note that Besson *et al.*[31,28] have suggested that most experimental transition pressures in III-V compounds quoted prior to their paper should probably be revised downward.

We predict a second-order or very weakly first-order rocksalt→*Cmcm* transition in the pressure range 110–120 kbar, the softness of the structure in this region making it very difficult to locate the transition pressure precisely (see Sec. IV E). Menoni and Spain[30] reported a transition from the rocksalt to the β-tin phase at about 190 kbar. We note that in preliminary work Nelmes *et al.*[3] have found no sign of a transition at 190 kbar, but have found indications of a ''*Cmcm*-like'' phase at about 340 kbar. This observation is in agreement with our predicted sequence of phase transitions, although the *Cmcm* phase was observed at pressures considerably above our calculated transition pressure. We predict further transitions from *Cmcm* InP to *Immm* at about 500 ± 20 kbar and then to the CsCl structure at 1020 ± 30 kbar, but there have been no experimental investigations reported in this high-pressure regime.

C. InAs

The phase diagram for InAs is similar to that for InP, and we predict the same sequence of stable phases. The zinc-blende→rocksalt coexistence pressure is calculated to be 39 kbar. The *Cmcm* distortion of the rocksalt structure appears in the pressure range 30–45 kbar, and therefore it is difficult to say whether there is any region of stability for the rocksalt structure at all. As in the case of InP, our calculated transition from rocksalt to *Cmcm* is predicted to be second order or extremely weakly first order. Experimentally a transition from zinc blende to rocksalt has been reported by Vohra *et al.* at 70 kbar.[32] Nelmes *et al.*[2] have reported a transition on increase of pressure at 70 kbar from the zinc-blende phase to a phase that appears to be a mixture of NaCl and other structures. They also reported the reverse transition on decreasing pressure at about 30 kbar. A reasonable approximation for the coexistence pressure is to take the mean value of this hysteresis range (50 kbar), which is in quite good agreement with our calculated value of about 40 kbar. A previous calculation of this transition pressure by Zhang and Cohen[29] yielded a value of 84 kbar, although we note again that these authors did not include nonlinear core-valence exchange-correlation corrections, so that this value is certainly too high. We have not found a thermodynamically stable sc16 phase for InAs.

Vohra *et al.* also reported a transition from rocksalt to a site disordered β-tin phase at 170 kbar.[32] We have not investigated site disordered structures, but our results indicate that the site-ordered β-tin structure is unstable towards the *Immm* structure (see Sec. IV F).

At higher pressures we predict transitions from *Cmcm* InAs to *Immm* at about 240 ± 25 kbar and then to the CsCl structure at 670 ± 12 kbar. No experimental investigations have been reported in this pressure regime.

D. General remarks on the phase stability

The energy-volume and enthalpy-pressure curves for GaAs (see Ref. 6) and GaP have similar forms, as do those for InP and InAs. Consequently, the phase diagrams of GaP and GaAs are similar, as are those of InP and InAs. These findings suggest a more important role for the cation than the anion in determining the high-pressure phase diagrams of these compounds. This behavior can be extended to the case

of AlX compounds, with X being As and P. For instance, in these materials there is experimental[33,34] and theoretical[6] evidence for the existence of a stable NiAs structure, whereas the NiAs structure is not even close to being stable in InX and GaX compounds.

We have found a pressure range (147–203 kbar) of thermodynamic stability for sc16-GaP. We found a similar situation in our previous work on GaAs,[6] although in that case the stability range was very small (117–125 kbar).[35] For InP and InAs we have not found stable sc16 phases. In fact, there have been no reports of a stable sc16 phase in any III-V compound. It has been suggested that the transition from the zinc-blende to the sc16 structure is strongly kinetically hindered.[10] The possibility of obtaining a stable sc16 structure in these compounds as pressure is increased from the zinc-blende phase or released from high-pressure phases remains an interesting question to be settled by experiments.

We have found stable $Cmcm$ phases in InP and InAs and a marginally stable $Cmcm$ phase in GaP. Although earlier experimental works did not report the existence of the $Cmcm$ phase, the results of the present work are in accord with the recent preliminary experimental investigations of Nelmes and co-workers.[2] According to our calculations and recent experiments,[1] in both InP and InAs the zinc-blende structure becomes unstable to the NaCl structure, which in turn becomes unstable to the $Cmcm$ structure. In the case of GaP and GaAs, the rocksalt structure is somewhat higher in enthalpy than the β-tin structure in the range of pressures where the zinc-blende structure becomes unstable and thus a thermodynamically stable rocksalt structure is not expected. However, when the $Cmcm$ distortion of the rocksalt structure is considered, the enthalpy is lowered and the $Cmcm$ structure is favored over the other structures considered. The E-V curves for the *Imm2* and $Cmcm$ phases are close at high pressures, which is somewhat surprising because the structures are not closely related.

It turns out that the much studied β-tin structure is mechanically unstable to a *Imm2* distortion at high pressure (see Sec. IV F). In particular, for InP and InAs, β tin is not mechanically stable in the whole range of positive pressures investigated. In view of these results we suggest that the stability of this structure should be reevaluated in all the binary compounds for which it has been proposed as a stable or nearly stable high-pressure phase. The only previous theoretical study of a *Imm2* structure of a III-V compound is the study of InSb by Guo *et al.*,[36] who found the β-tin phase to be unstable to the *Imm2* phase, with the v structural parameter being very close to 0.5 at all pressures. Experimentally an $Immm$ phase has been observed in InSb (Ref. 37), and an *Imm2* phase has been reported in GaAs.[19] Further experimental work aimed at observing $Immm$-like phases in other III-V compounds would be valuable.

E. Instability of the rocksalt structure to a *Cmcm*-type distortion

In order to investigate the mechanism leading to the distortion from rocksalt to $Cmcm$ we have performed calculations at fixed volume imposing separately on the rocksalt structure each of the three components of the distortion [the shearing of the alternate (001) planes u, the puckering of the atomic rows δ, and the orthorhombic distortion of the cell]. The rocksalt structure turns out to be stable to the cell distortion and the puckering alone, but is unstable at reduced volumes to the shearing of the (010) planes. In Fig. 8(a) we show the energy obtained when a shear u is imposed on the rocksalt structure of InP, while keeping the form of the cell fixed and not allowing for puckering of the atomic rows. Each curve corresponds to a different fixed volume and the energy is measured with respect to the energy of the rocksalt structure at that volume. While the rocksalt structure is stable to the shearing distortion at large volumes, it becomes unstable as the volume decreases. The different contributions to the total energy corresponding to this shearing-only deformation are plotted in Fig. 8(b), for the volume 0.632 $V_{0,\mathrm{the}}^{\mathrm{InP}}$, where ''the'' denotes theoretical value.[38] At this volume the rocksalt structure is already mechanically unstable to shearing. As can be seen, the main terms in the total energy leading to the distortion are the ion-ion energy ($E_{i\text{-}i}$) and the kinetic energy (E_{kin}), which strongly favor the structures with u close to 0.5. The Hartree term E_H further favors the distortion, but a delicate cancellation with the rest of the terms (the exchange-correlation energy E_{xc} and the electron-ion interaction $E_{e\text{-}i}$), which tend to stabilize the rocksalt structure, produces the minimum in the total-energy curves shown in the graph. The distance between the ions increases with the $Cmcm$ distortion, so that the packing is more efficient than the NaCl structure. Consequently, the Ewald energy of the $Cmcm$ structure is lower than that of NaCl.

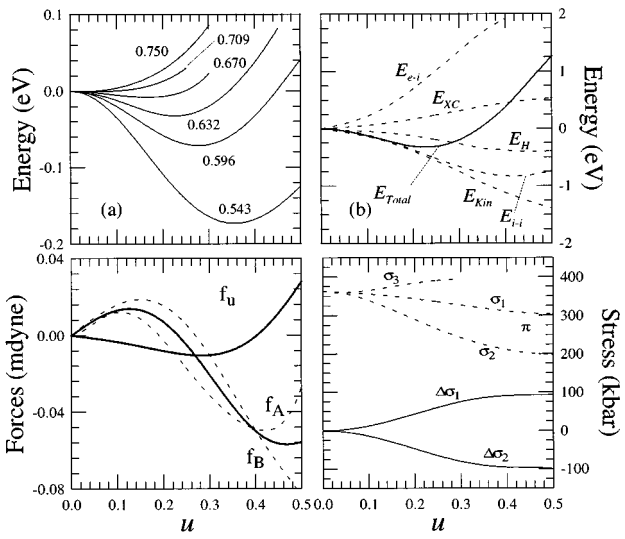

FIG. 8. (a) Change in energy of InP when a shearing of alternate (010) planes by $\frac{1}{2}uc$ is imposed on the rocksalt structure, while not allowing for further deformations of the cell or the atomic chains. Each curve corresponds to a different fixed volume. The energy is measured in eV per formula unit. (b) Different contributions to the total energy measured wih respect to the values for the rocksalt structure. The total energy is also shown, multiplied by 10 in order to make it representable on the scale. (c) Forces on each atomic species (f_A and f_B) and generalized forces associated with the shearing parameter (f_u) and with the puckering parameter (f_δ). (d) Components of the stress tensor (σ_1, σ_2, and σ_3), and generalized forces associated with the axial ratios b/a and c/a ($\Delta\sigma_1$ and $\Delta\sigma_2$) and with the volume (π). (b)–(d) correspond to the volume $V=0.632V_{0,\mathrm{the}}^{\mathrm{InP}}$.

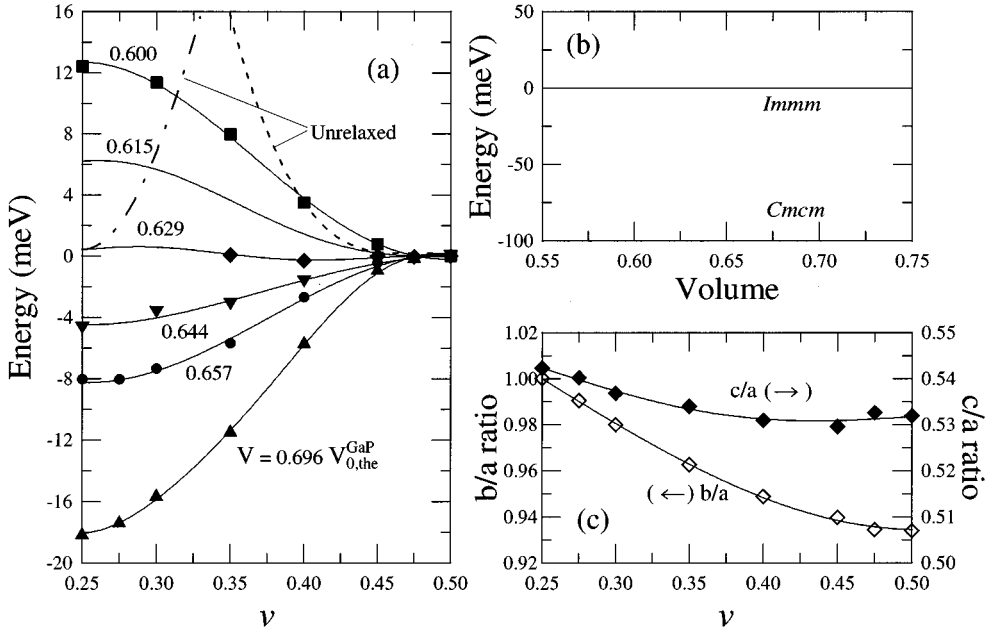

FIG. 9. (a) Energy curves of the *Imm2* structure of GaP as a function of the internal parameter v. Each solid curve corresponds to a different fixed volume. At each volume and v, the b/a and c/a ratios have been relaxed. The different symbols represent the calculated energies at each volume [in meV per formula unit with respect to the energy of the *Immm* structure ($v=0.5$)]. The two curves labeled ''unrelaxed'' correspond, respectively, to fixing the values of both b/a and c/a to those for the relaxed β tin (left curve) and *Immm* (right curve) structures. (b) Energy of the *Immm* and *Cmcm* structures with respect to the β-tin structure, as a function of the volume for GaP (solid lines), InP (dashed lines), and InAs (dash-dotted lines). (c) The b/a and c/a ratios of the relaxed *Imm2* structure at the volume $V=0.629V_{0,\mathrm{the}}^{\mathrm{GaP}}$, as a function of the internal parameter v.

Moreover, as the *Cmcm* distortion increases the bonds become less well defined and the charge density becomes smoother, i.e., the system becomes more free-electron-like and the kinetic energy is lowered. At low pressures the NaCl structure is stabilized by strong interatomic bonding, but at higher pressures the packing constraints become more important. The main features of this picture remain unchanged when the full cell relaxation is considered.

The analysis of the forces on the atoms and the stress on the cell that appear on shearing of the (010) planes reveals the origin of the further distortions that lead to the *Cmcm* structure. This analysis is shown in Figs. 8(c) and 8(d). The forces f_u and f_δ depicted in Fig. 8(c) are the generalized forces related, respectively, to the shearing parameter u and to the puckering parameter δ, which can be obtained from the calculated Hellmann-Feynman forces on each atomic species f_A and f_B.[39] Figure 8(d) shows the diagonal components of the stress tensor σ_{11}, σ_{22}, and σ_{33}, related to the x, y, and z directions, respectively. The ''anisotropy'' in the diagonal components of the stress tensor $\Delta\sigma_1=\frac{1}{3}(2\sigma_{22}-\sigma_{33}-\sigma_{11})$ and $\Delta\sigma_2=\frac{1}{3}(2\sigma_{33}-\sigma_{22}-\sigma_{11})$ are the generalized forces related to the cell shape parameters at fixed volume, namely, the axial ratios b/a and c/a. (A positive value of these forces means a decrease in energy if the corresponding axial ratio increases.) The values of the generalized force related to the volume [the pressure $\pi=\frac{1}{3}(\sigma_{11}+\sigma_{22}+\sigma_{33})$], $\Delta\sigma_1$, and $\Delta\sigma_2$ are also depicted in Fig. 8(d). At the reduced volume considered in these figures, we see that a shearing u produces a positive (i.e., nonrestoring) force f_u. A force f_δ also arises, which causes the puckering of the atomic rows. Finally, the non-negligible values of $\Delta\sigma_1$ and $\Delta\sigma_2$ induced by the shearing tend to deform the cell by increasing b/a and decreasing c/a with respect to the rocksalt values $b/a=c/a=1$. These tendencies are in agreement with the values of the parameters for the fully relaxed *Cmcm* structure at this volume (see Sec. V). Also note that the shearing reduces the pressure π and thus further lowers the enthalpy of the distorted phase with respect to the rocksalt structure.

F. Stability of *Imm2*

We have also considered in detail the case of the *Imm2* structure for these compounds. In order to investigate the stability of the *Imm2* structure we have performed calculations on *Imm2* at different volumes, fixing the value of the internal parameter v within its range of variation 0.25–0.5 and relaxing the shape of the orthorhombic cell at fixed volume and v.

The energies obtained in this way for GaP are plotted in Fig. 9(a), where the different symbols represent our calculated values at a certain fixed volume. In Fig. 9(b) we plot the energy difference between the *Immm* ($v=0.5$) and β-tin ($v=0.25$ and $b/a=1$) structures as a function of volume. (Also shown for the sake of completeness is the difference in energy between the *Cmcm* and β-tin structures.) Finally, Fig. 9(c) shows the axial ratios b/a and c/a corresponding to the shape-relaxed structures as a function of the internal parameter v, for the volume $V=0.629V_{0,\mathrm{the}}^{\mathrm{GaP}}$.

Figure 9(c) is illustrative of our results for the cell shape relaxation. We note that at $v=0.25$ the minimum-energy structure corresponds, in all cases investigated, to the β-tin

structure; that is, upon relaxation of the axial ratios of the *Imm2* structure with $v=0.25$, we find $b/a=1$. This means that the tetragonal β-tin structure is stable against a purely orthorhombic distortion of the cell. However, it is not always stable against a more general *Imm2* distortion, as will be shown. We also note that the (nonzero) slope of both the (b/a)-v and the (c/a)-v curves at $v=0.25$ is accounted for by the symmetry properties of the *Imm2* structure discussed in Sec. II B,[40] as is the zero slope of these curves at $v=0.5$.

At each fixed volume, symmetry considerations ensure that the E-v curves plotted in Fig. 9(a) have either maxima or minima at both $v=0.25$ and $v=0.5$, the extrema of the interval of variation of v. At large volumes, $v=0.25$ corresponds to a minimum in the energy and $v=0.5$ corresponds to a maximum, as shown in the figure. Thus the β-tin structure is the mechanically stable *Imm2* structure at large volumes (and correspondingly low pressures). As the volume decreases, the difference in energy between the maximum at $v=0.5$ and the minimum at $v=0.25$ decreases. At a volume of approximately $V_c=0.630V_{0,\mathrm{the}}^{\mathrm{GaP}}$ both the β-tin structure and *Immm* structures have the same energy [see Fig. 9(b)]. Around this volume, the E-v curves depicted in Fig. 9(a) are essentially flat. As the volume is further reduced, the energy of the *Immm* structure becomes lower than that of the β-tin structure. The *Immm* structure ($v=0.5$) corresponds now to a minimum in the E-v curve and is the stable *Imm2* structure. The extremum at $v=0.25$ has turned into a maximum of the E-v curve. Thus the β-tin structure becomes mechanically unstable at low volumes, at which the stable *Imm2* structure is *Immm*.

We could not locate a maximum or minumum, other than those at $v=0.25$ and $v=0.5$, for any of the E-v curves shown in Fig. 9(a), each corresponding to a different volume. An extremum could exist at some v between 0.25 and 0.5 for volumes close to V_c, where the E-v curves are very flat, but it must be extremely shallow (well below 1 meV per formula unit). On account of this extremely small difference in energy between structures with different v near the onset of the mechanical instability of the β-tin structure, the vibrational degrees of freedom of the crystal could play an important role in stabilizing the actual stable structure. Thus there could be a small region of stable *Imm2* structures with v in the range 0.25–0.5, near the pressure of coexistence of the β-tin and *Immm* structures ($\sim$ 390 kbar).

We stress the importance of the cell-shape relaxation in *Imm2*. This is shown by the two dashed curves in Fig. 9(a), which represent the energy obtained by varying v while keeping the shape of the cell fixed to that of the fully relaxed *Imm2* structure at either $v=0.25$ (left dashed curve) or $v=0.5$ (right dashed curve), for the volume $V=0.629V_{0,\mathrm{the}}^{\mathrm{GaP}}$. The rapid growth of these energy curves away from $v=0.25$ and $v=0.5$, respectively, is in sharp contrast to the rather flat behavior of the energy curve for the cell-shape relaxed structure at this volume.

For InP and InAs [see Fig. 9(b)] we find that, in the range of positive pressures investigated, the E-v curves for *Imm2* always have a unique minimum at $v=0.5$ and a unique maximum at $v=0.25$, i.e., we find that *Immm* is always favored over the more general *Imm2* structure and also that the β-tin structure is not mechanically stable at any positive pressure. This result is in line with previous calculations for InSb.[36]

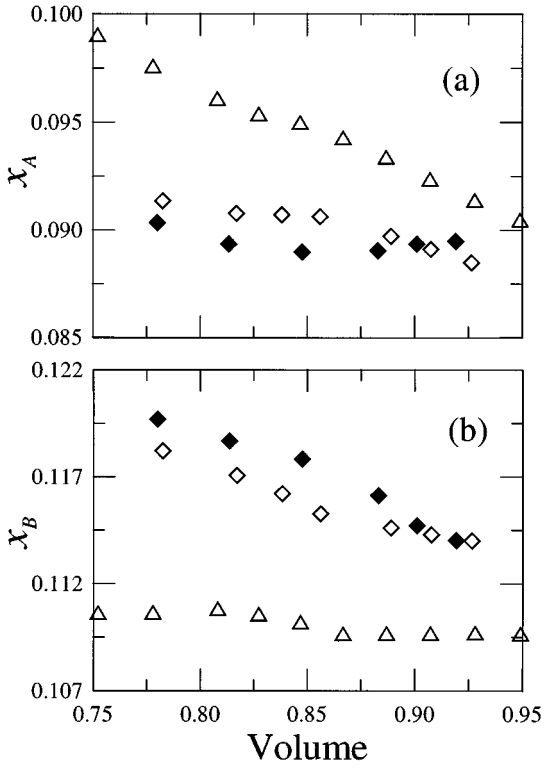

FIG. 10. x_A (Ga/In) and x_B (P/As) internal parameters for the relaxed sc16 structure of the three compounds, as a function of volume (normalized to the calculated equilibrium volume of the zinc-blende phase). The symbols correspond to GaP (triangles), InP (diamonds), and InAs (filled diamonds).

V. STRUCTURAL PARAMETERS

In this section we present the calculated values of the structural parameters for the relaxed sc16, *Cmcm*, and *Immm* structures. At the moment there is no experimental data with which to compare these values. However, the values given here may help in the identification of phases in experimental data. Moreover, the present level of accuracy of high-pressure x-ray-diffraction experiments[3] should make it possible to study experimentally the evolution of the structural parameters with pressure in some cases, which will allow for a very detailed comparison between theory and experiment.

In Fig. 10 we show values of the x_A (Ga/In) and x_B (P/As) internal parameters, defined in Ref. 6, for the sc16 phases of GaP, InP, and InAs as a function of volume. (A similar plot for sc16-GaAs was given in Ref. 6.) As was previously found for GaAs, the internal parameter related to the anion is larger than for the cation. At zero pressure we obtain $x_{\mathrm{Ga}}=0.0924$ and $x_{\mathrm{P}}=0.1097$ (GaP), $x_{\mathrm{In}}=0.0891$ and $x_{\mathrm{P}}=0.1144$ (InP), and $x_{\mathrm{In}}=0.0893$ and $x_{\mathrm{As}}=0.1147$ (InAs) [cf. the experimental zero pressure value of the internal parameter x of about 0.1025 in bc8 Si (Ref. 41) and our calculated value of 0.1020 (Ref. 12).

The structural parameters of the *Cmcm* phases are of par-

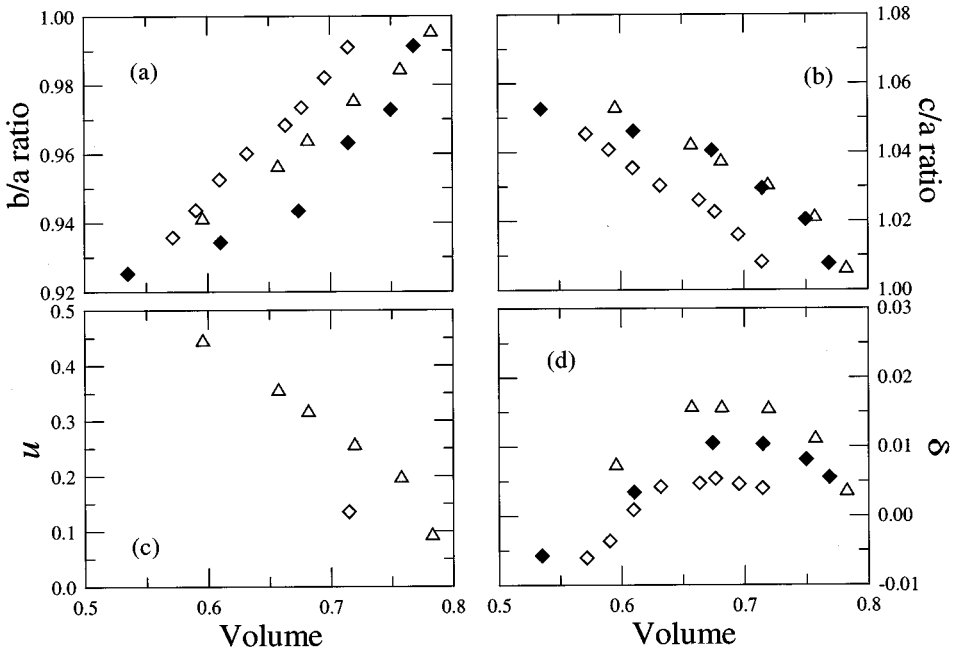

FIG. 11. Volume dependence of the structural parameters of the relaxed *Cmcm* structure of GaP (triangles), InP (diamonds), and InAs (filled diamonds). The volume is given in terms of the calculated zero-pressure volume of the zinc-blende phase of each compound.

ticular importance as this phase could be stable in each of the compounds studied. In Figs. 11(a)–11(d) we plot the values of b/a, c/a, u, and δ as a function of volume. Note that at volumes close to the onset of the instability of rocksalt to the *Cmcm* distortion (the higher volumes plotted) the structure is very soft and the determination of the parameter values is difficult. Consequently, our results at large volumes are less precise than those at small volumes. As the volume increases, the *Cmcm* distortion of the rocksalt cell tends to disappear and thus the magnitude of both the b/a and c/a ratios tend to 1 and the shearing and puckering parameters u and δ tend to 0, leading to the rocksalt structure. On the other hand, the trend is that b/a decreases and c/a increases from the rocksalt value of 1 as the volume is reduced. As noted in Sec. IV E these tendencies are in agreement with the analysis of the generalized forces related to these parameters, which arise when a pure shearing is imposed on the rocksalt structure. The shearing distortion from the rocksalt structure increases as the pressure increases. The values of the puckering parameter δ seem to be, in all cases, rather small. [Compare these calculated values with the experimental value of 0.06 in the case of CdTe at about 186 kbar (Ref. 3).]

The variation with volume of the c/a and b/a ratios for the *Immm* structures are shown in Figs. 12(a)–12(b), respectively. Also shown, for the sake of comparison, is the variation of the c/a ratio of the β-tin structure of GaP. The c/a ratios decrease as the pressure is increased, whereas the b/a ratios tend to increase with increasing pressure. Note that at a pressure of about 250 kbar our calculated b/c ratio for *Immm* GaP is approximately equal to $\sqrt{3}\approx 1.732$, for which the arrangement of the *sites* is the same as in the monatomic simple hexagonal structure (see Sec. II). In the range of pressures 160–700 kbar (~ 0.70–$0.55 V_{0,\mathrm{the}}^{\mathrm{GaP}}$) the b/c ratio of *Immm* GaP increases from about 1.70 to 1.77 and thus it differs only by a few percent from this special value.

VI. CONCLUSION

Our understanding of the high-pressure phase diagrams of III-V compounds is undergoing a period of rapid evolution. The important different point is that the relatively high-symmetry rocksalt and β-tin phases, which were once thought to be common among the high-pressure phases of III-V and II-VI compounds, are often unstable to symmetry lowering distortions.

In the present study we have included several phases of GaP, InP, and InAs that have not been studied previously. We have considered in detail the *Cmcm* and *Imm2* struc-

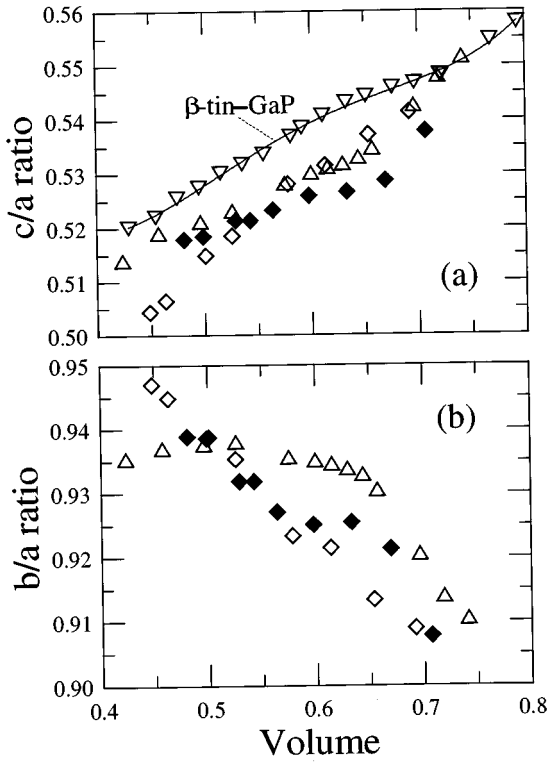

FIG. 12. Same as Fig. 11, but for the c/a and b/a ratios of the *Immm* structure of GaP (triangles), InP (diamonds), and InAs (filled diamonds). The c/a ratio for the β-tin structure is also shown in (a) (downward triangles and solid curve).

tures, which are symmetry lowering distortions of the rocksalt and β-tin structures, respectively. Together with our previous work on GaAs (Ref. 6) we now have enough results to start to put together a different systematics of the high-pressure phases of III-V compounds.

We have found stable *Cmcm* phases in GaAs, InP, and InAs and a stable or nearly stable *Cmcm* phase in GaP. The rocksalt structure is predicted not to be stable at any pressure in GaP and GaAs, while in InP and InAs there is a pressure region where it is stable. These findings are in line with recent experimental investigations by McMahon and Nelmes.[1] The driving force for the instability of the rocksalt structure to the *Cmcm* distortion is the shearing of alternate (010) planes in the [001] direction.

Our results indicate that stable *Imm2*-like phases could be observed experimentally at higher or even similar pressures to those at which the *Cmcm* phases are expected to be stable. For the two In*X* compounds considered here we have found that the *Immm* structure (i.e., *Imm2* with $v=0.5$) is mechanically stable in the whole range of positive pressures investigated. For GaP there is a range of lower positive pressures where the β tin structure is mechanically stable. At higher pressures β-tin becomes unstable. At pressures around the onset of the instability of β-tin GaP, a continuum of *Imm2* structures could exist, with v increasing within the range from 0.25 to 0.5 as pressure increases. At high pressures *Immm* GaP ($v=0.5$) is favored.[35] We emphasize that the *Imm2*-like phases in our calculations are very stable in the sense that their enthalpies are considerably below those of the other phases at some pressures. Further experimental work is required at the more elevated pressures at which *Imm2* phases are predicted to be stable.

We have also considered the issue of the stability of a sc16 phase in these compounds. Our calculations indicate that sc16 is not thermodynamically stable in either InP or InAs, but we do find a range of thermodynamical stability for sc16 GaP, as we found previously for sc16 GaAs.[6] Although it may well be possible that a direct zb$\rightarrow$sc16 transition does not occur, it is nevertheless interesting that there is a predicted range of thermodynamical stability for both sc16 GaP and sc16 GaAs.

A different systematics of the high-pressure phase diagrams of III-V compounds is now under construction. This area of high-pressure research is producing different and exciting results that are fostering a stimulating interplay between theory and experiment.

ACKNOWLEDGMENTS

We acknowledge fruitful discussions with R. J. Nelmes, M. I. McMahon, S. A. Belmonte, and A. Muñoz. We thank J. M. Besson for bringing Ref. 30 to our attention. This work was supported by the Engineering and Physical Sciences Research Council (United Kingdom). A.M. acknowledges partial financial support from the Ψ_k HCM Network (Contract No. ERBCHRXCT930369).

[1] M.I. McMahon and R.J. Nelmes, J. Phys. Chem. Solids **56**, 485 (1995).

[2] R.J. Nelmes, M.I. McMahon, N.G. Wright, D.R. Allan, H. Liu, and J.S. Loveday, J. Phys. Chem. Solids **56**, 539 (1995).

[3] R.J.Nelmes, M.I. McMahon, N.G. Wright, and D.R. Allan, Phys. Rev. Lett. **73**, 1805 (1994); Phys. Rev. B **51**, 15 723 (1995).

[4] R.J. Nelmes and M.I. McMahon, Phys. Rev. Lett. **74**, 106 (1995).

[5] R.J. Nelmes and M.I. McMahon (private communication).

[6] A. Mujica, R.J. Needs, and A. Muñoz, Phys. Rev. B **52**, 8881 (1995).

[7] A. Mujica and R.J. Needs, J. Phys.: Condens. Matter **8**, L237 (1996).

[8] G.-D. Lee and J. Ihm, Phys. Rev. B **53**, 7622 (1996).

[9] R.J. Nelmes, M.I. McMahon, P.D. Hatton, J. Crain, and R.O. Piltz, Phys. Rev. B **47**, 35 (1993).

[10] J. Crain, R.O. Piltz, G.J. Ackland, S.J. Clark, M.C. Payne, V. Milman, J.S. Lin, P.D. Hatton, and Y.H. Nam, Phys. Rev. B **50**, 8389 (1994); **52**, 16 936(E) (1996).

[11] J.S. Kasper and S.M. Richards, Acta Crystallogr. **17**, 752 (1964).

[12] R.J. Needs and A. Mujica, Phys. Rev. B **51**, 9652 (1995).

[13] A. Mujica and R.J. Needs, Phys. Rev. B **48**, 17 010 (1993).

[14] R.W.G. Wyckoff, *Crystal Structures* (Interscience, New York, 1963).

[15] Note also that the structure resulting from interchanging the positions of the unlike atoms 3 and 4 of the basis [see Fig. 1(b)] corresponds to changing u_A and u_B to $1-u_A$ and $1-u_B$, respectively. This fact allows us to study the energetics of the ''reordered structure'' using the same representation as the ''normal structure.'' We find this reordered structure, with like nearest neighbors, to be unfavorable with respect to the normal one.

[16] C.A. Vanderborgh, Y.K. Vohra, and A.L. Ruoff, Phys. Rev. B **40**, 12 450 (1989).

[17] S.B. Zhang and M.L. Cohen, Phys. Rev. B **39**, 1450 (1989).

[18] S.T. Weir, Y.K. Vohra, C.A. Vanderborgh, and A.L. Ruoff, Phys. Rev. B **39**, 1280 (1989).

[19] D.M. Ceperley and B.J. Alder, Phys. Rev. Lett. **45**, 566 (1980), as parametrized by J.P. Perdew and A. Zunger, Phys. Rev. B **23**, 5048 (1981).

[20] D. Hamann, M. Schlüter, and C. Chiang, Phys. Rev. Lett. **43**, 1494 (1979),

[21] G. Kerker, J. Phys. C **13**, L189 (1980).

[22] S.G. Louie, S. Froyen, and M.L. Cohen, Phys. Rev. B **26**, 1738 (1982).

[23] S. Froyen and M.L. Cohen, Phys. Rev. B **28**, 3258 (1983).

[24] H.J. Monkhorst and J.D. Pack, Phys. Rev. B **13**, 5189 (1976).

[25] O.H. Nielsen and R.M. Martin, Phys. Rev. B **32**, 3780 (1985); **32**, 3792 (1985).

[26] A. García and M.L. Cohen, Phys. Rev. B **47**, 6751 (1993).

[27] M. Baublitz and A.L. Ruoff, J. Appl. Phys. **53**, 6179 (1982).

[28] J.M. Besson (private communication); G. Weill, J.C. Chervin, and J.M. Besson, High Pressure Res. **7**, 105 (1991).

[29] S.B. Zhang and M.L. Cohen, Phys. Rev. B **35**, 7604 (1987).

[30] C.S. Menoni and I.L. Spain, Phys. Rev. B **35**, 7520 (1987).

[31] J.M. Besson, J.P. Itié, G. Weill, J.L. Mansot, and J. Gonzalez, Phys. Rev. B **44**, 4214 (1991).

[32] Y.K. Vohra, S.T. Weir, and A.L. Ruoff, Phys. Rev. B **31**, 7344 (1985).

[33] R.G. Greene, H. Luo, T. Li, and A.L. Ruoff, Phys. Rev. Lett. **72**, 2045 (1994).

[34] R.G. Greene, H. Luo, and A.L. Ruoff, J. Appl. Phys. **76**, 7296 (1994).

[35] We have also extended our previous study of GaAs (Ref. 6) to include the *Imm2* structure, and we now predict that a stable *Immm* phase exists in GaAs, between the β tin and CsCl phases. This further emphasizes the similarities between the phase diagrams of GaP and GaAs.

[36] G.Y. Guo, J. Crain, P. Blaha, and W.M. Temmerman, Phys. Rev. B **47**, 4841 (1993).

[37] R.J. Nelmes, M.I. McMahon, N.G. Wright, D.R. Allan, and J.S. Loveday, Phys. Rev. B **48**, 9883 (1993).

[38] $E_{\text{total}}=E_{\text{kin}}+E_{e\text{-}i}+E_H+E_{\text{xc}}+E_{i\text{-}i}$.

[39] Through the definition of u and δ in terms of the internal parameters for each atomic species u_A and u_B, we have $f_u=\frac{1}{2}(f_A+f_B)$ and $f_\delta=\frac{1}{2}(f_A-f_B)$. Here f_A and f_B are the z components of the forces on atoms 3 and 4 of the basis, of species A and B, respectively.

[40] The *Imm2* structure defined by $v=0.25+\epsilon$, a, b, and c is the same as $v'=0.25-\epsilon$, $a'=b$, $b'=a$, and $c'=c$.

[41] J. Crain, G.J. Ackland, J.R. Maclean, R.O. Piltz, P.D. Hatton, and G.S. Pawley, Phys. Rev. B **50**, 13 043 (1994).

[42] *Semiconductors, Physics of Group IV Elements and III-V Compounds*, edited by O. Madelung, Landolt-Börnstein, New Series, Group III, Vol. 17, pt. a (Springer-Verlag, Berlin, 1982).